Transient Kinetic Studies of the Formation of Primary Olefins from Dimethyl Ether over ZSM-5 Catalysts

Toyin Omojola[1,2,*], Dmitry B. Lukyanov[1] and Andre C. van Veen[2,*]

[1] Department of Chemical Engineering. University of Bath. Bath. BA2 7AY. UK

[2] School of Engineering. University of Warwick. Coventry. CV4 7AL. UK

***** Correspondence: o.omojola@bath.ac.uk, andre.vanveen@warwick.ac.uk

Abstract

The formation of primary olefins from dimethyl ether (DME) was studied over ZSM-5 catalysts at 300 °C using a novel step response methodology in a temporal analysis of products (TAP) reactor. To analyse the experimental results quantitatively, a kinetic model was developed and the kinetic parameters were obtained by solving a plug flow reactor model with coupled convection, adsorption, desorption, and reaction steps. Propylene was observed as the major primary olefin and portrayed an S-shaped profile with preceding induction period when it was not observed in the gas phase. Methanol and water portrayed overshoot profiles due to their different rates of generation and consumption. Initially, DME effluent shows a rapid rise half-way to its steady state value followed by a slow rise thereafter. This was explained by a fast rate of reaction between surface methoxy groups ($CH_3{\cdot}Z$) and methanol followed by subsequent reactions involving DME in further steps during the induction period. The experimental data and their analysis suggest that the major bottleneck involved in propylene generation is the formation of the first C-C bond from the reaction between methoxymethyl groups ($CH_3OCH_2{\cdot}Z$) and DME. DME adsorption on ZSM-5 catalyst generates surface methoxy groups which further react with the feed to give methoxymethyl groups. These methoxymethyl groups are regenerated through a series of reactions involving intermediates such as dimethoxymethane and methyl propenyl ether before propylene formation. In effect, the reaction is autocatalysing as readily shown by the S-shaped propylene profile.

Keywords: induction period; hydrocarbon pool; dimethyl ether (DME); temporal analysis of products (TAP) reactor; ZSM-5 zeolite; transient kinetics; primary olefins; step response; surface methoxy groups; methoxymethyl groups; methanol

1. Introduction

An increasing demand of highly-valuable chemicals and their security as well as incentives to reduce the carbon footprint needed for their generation and utilization all make the conversion of methanol to olefins (MTO) a viable chemical process. Non-conventional feedstock (such as biomass) or highly abundant conventional resources (such as coal) are used to produce methanol which can later be transformed to olefins over zeolite catalysts (1).

The production of hydrocarbons from methanol (MTH) under steady-state conditions is regulated by a well-established “hydrocarbon pool” mechanism also known as the dual-cycle consisting of an olefin and aromatic cycle over ZSM-5 catalysts (2-6). The propagation of both cycles over the ZSM-5 catalyst is tunable depending on process conditions (7).

Methanol undergoes a rapid equilibration process over ZSM-5 catalysts leading to the formation of dimethyl ether (DME) and water (8). There exists a long standing scholarly debate on the evolution of the key oxygenate (methanol and/or DME) into the steady-state hydrocarbon pool mechanism. This debate centers on: (a) the role of methanol and/or DME, (b) the primary olefin(s) formed (ethylene only, propylene only or ethylene and propylene) and (c) the dominant mechanism leading from the key oxygenate to the primary olefin.

Various mechanisms have been proposed for the conversion of methanol/DME to primary olefins (9). Using Density Functional Theory (DFT) calculations, Lesthaeghe et al. (10-12) refuted some direct mechanisms based on high activation energy barriers and highly unstable intermediates. Olefins have been also proposed to form indirectly from impurities (acetone, ethanol) in the methanol feed (13, 14). However, Hunger and co-workers (15-17) observed that the quantity of impurities proposed were insufficient for primary olefin formation. Recently, there has been a surge in the evidence for the direct mechanism leading to primary olefin formation (18-20). Li et al. (20) gave evidence, using DFT calculations, for the formation of propylene from methanol through methoxymethyl cations. In this pathway, 1,2-dimethoxyethane or 2-methoxyethanol were proposed as key intermediates propagating the direct formation of propylene.

Although theoretical calculations have shown the feasibility of direct pathway involving methoxymethyl cations for the direct formation of ethylene and propylene from methanol, there are no studies to experimentally validate these proposals. Moreover, there is no model developed on a microscale level to describe and predict the formation of primary olefins from oxygenates particularly in the induction period.

Recently, we observed that higher temperatures are required to desorb DME compared to methanol providing evidence that DME stays longer on the catalysts (21) and is the key oxygenate in surface reactions. This was earlier evidenced by Liu et al. (19) and Wei et al. (22). In this paper, we investigate the induction period during which DME is transformed to

primary olefins at 300 °C by conducting transient kinetic studies in a temporal analysis of products (TAP) reactor. Using the theoretical pathway described by Li et al. (20) as a basis of a reaction scheme for a microkinetic model, the experimental data was simulated to extract kinetic parameters that describe the formation of primary olefins from DME over fresh ZSM-5 catalysts.

2. Experimental

The ammonium form of the fresh ZSM-5 catalyst with a Si/Al ratio of 25, purchased from Zeolyst International was pressed, crushed, and sieved to obtain particles sizes in the range of 250 – 500 µm. Anhydrous DME (99.999%) and argon (99.999%) were purchased from CK special gases Ltd. Experiments were conducted in a transient reactor suited for the temporal analysis of products (TAP). The TAP has three chambers in series: (a) the reactor chamber, (b) the differential chamber and (c) detector chamber. The reactor chamber contains a fixed-bed reactor, 6 mm O.D. (4 mm I.D.) and 40 mm long and has a cone-shaped inset for uniform radial distribution. The differential chamber acts as a cryogenic trap to eliminate scattered molecules reaching the detector chamber where the quadrupole mass spectrometer (QMS) is housed. In effect, the differential chamber works as a molecular beam (23).

Gases were introduced through two continuous feeding valves into the reactor inlet. The pressure at the exit of the reactor chamber is maintained at 10^{-5} Pa while the pressure at the end of the differential chamber is 10^{-6} Pa and QMS is 10^{-7} Pa. The response of the QMS, placed in the detector chamber, was calibrated by passing continuous streams of various gases (methanol, DME, propylene, etc.) in argon over an inert quartz bed with particle diameters between 355 – 500 µm. The QMS was operated in a multiple ion detection (MID) mode. The low base pressure (10^{-7} Pa) in the detector chamber allows for high detection sensitivity necessary for quantitative analysis. The inert quartz bed used for calibration had the same length as the catalyst bed. The time required to reach steady state or to drop from steady state was fastest over the inert quartz bed.

10 mg of NH_4-ZSM-5 catalyst was initially decomposed in the TAP reactor chamber by heating it at 10 °C min^{-1} up to 450 °C, holding for 30 min before bringing the sample to 300 °C. Background signal intensities were then obtained. The catalyst was then subjected to a steady flow of argon at 10^{-8} mol s^{-1}. Afterwards, the flow was instantaneously switched to a feed of 5 vol% DME in argon (step-up) at a flow rate of *ca*. 4.40×10^{-8} mol s^{-1}. During the step response cycle, the effluent was continuously monitored with the QMS.

Flow rates of the inert feed were similar to step response feed and were about 10^{-8} mol s^{-1}, with an inlet pressure of less than 1000 Pa (24). The active catalyst bed length was short (2 mm) compared to the overall bed length of 25 mm (consisting of quartz wool/quartz

beads/catalyst bed/quartz beads/quartz wool). Hence, a thin-zone configuration was realised which removes concentration gradients along the bed while achieving high conversions (25). The level of non-uniformity in a thin-zone TAP reactor is lower than 20% for conversions up to 75% and only becomes significant for conversions above 80% (26).

Throughout all step response experiments, the temperature and the pressure were constant, and the experiments were repeated severally to check for reproducibility. The raw data (QMS ion currents) were corrected for background levels and fragmentation contributions for the different molecules and sensitivity factors.

Steady state DME conversion was calculated using equation 2.1 below:

$$X_{DME} = \frac{2\dot{n}_{DME,i} - \left(\dot{n}_{MeOH,e} + 2\dot{n}_{DME,e}\right)}{2\dot{n}_{DME,i}} \quad (2.1)$$

Where X_{DME} is the conversion of DME, $\dot{n}_{DME,i}$ is the molar feed flowrate of DME, $\dot{n}_{MeOH,e}$ is the effluent molar flowrate of methanol and $\dot{n}_{DME,e}$ is the effluent molar flowrate of DME.

3. Kinetic modelling

To obtain estimates of the kinetic parameters, the reactor performance was simulated. The outlet concentrations of methanol, DME, water and propylene were estimated using the measured inlet conditions of DME in a step function as a boundary condition. Rate parameters were estimated by comparing experiment to model. A one-zone plug flow reactor model was applied (27):

Gas

$$\varepsilon_b \frac{\partial C_{i,g}}{\partial t} = -u \frac{\partial C_{i,g}}{\partial z} - \Gamma_t S_v (1 - \varepsilon_b) k_{i,g} C_{i,g} \quad (2.2)$$

where $C_{i,g}$ is the concentration of specie i in the gas phase, mol m^{-3}; ε_b is bed porosity; u is the superficial velocity, m s^{-1}; z is the bed length, m; t is time, s; Γ_t is the concentration of active sites per unit surface area of catalyst (mol m_{cat}^{-2}) and S_v is the catalyst surface area per unit volume (m_{cat}^{-1})

Surface

$$\frac{\partial \theta_i}{\partial t} = k_{i,s} \theta_{i,s} \quad (2.3)$$

where θ_i is the surface coverage of specie i. Initial condition: t = 0, $C_{i,g}$ = 0, θ_i = 0. Boundary condition: (at t>0, z=0), C_i (0, t) = f(t)

The reactor model was solved in MATLAB (version R2016b) using the upwind scheme for solving the hyperbolic 1st order partial differential equation (PDE). Backward differencing was applied to the convection term in the PDE. It was assumed that surface diffusion of species in the pore is negligible and axial and radial dispersion are negligible given that the step response study was carried out with the continuous feeding valves of the TAP reactor.

The upwind scheme is stable if the Courant-Friedrichs-Lewy (CFL) condition (28) is satisfied (equation 2.4):

$$CFL = \left| a \frac{\Delta t}{\Delta z} \right| \leq 1 \qquad (2.4)$$

where a = u/ε_b. In our simulations, the time domain was divided into 4,000,000 strips and the length domain was divided into 10 strips such that CFL was 0.02426 which fulfils the CFL stability condition of the upwind scheme.

The sum of square error (SSE) between experiment and model was obtained according to:

$$\sum_n \sum_i \left(Y_{expt,i} - Y_{model,i}\right)^2 \rightarrow min \qquad (2.5)$$

where $Y_{expt,\,i}$ is experimental data of specie, i at time, t and $Y_{model,i}$ is the simulated data of specie, i at time, t.

Furthermore, to assess the sensitivity coefficients, the initial rate constants of each elementary step was multiplied by perturbation factors while other rate constants were kept constant. The relative changes in the sum of square error between the experimental and model were obtained with or without the perturbation factor. Subsequently, the sensitivity coefficient was obtained according to:

$$K_s = \frac{\ln(Y_p/Y_o)}{\ln(F)} \qquad (2.6)$$

where Y_p and Y_O are the SSE values with or without the perturbation factor and F is the perturbation factor.

The initial parameter estimates were improved greatly by reducing the sum of squares error between model and experiment. Parameter optimisation through the minimisation of the sum of square error using an “fminsearch” function was implemented in MATLAB (version R2016b). The “fminsearch” function uses a Nelder-Mead simplex algorithm as described in detail by Lagarias et al. (29).

4. Results

4.1. Step response study

Propylene is the major olefin formed at 300 °C over ZSM-5 catalysts in the TAP reactor. No ethylene effluent was observed in the gas phase. An induction period of 40 min occurs before the rise of propylene effluent (Fig. 2.1). During this induction period, water is generated and released in the gas phase and consumed until steady-state effluent values are reached. The water effluent portrays a stark overshoot profile. Methanol effluent mirrors this overshoot behaviour although its features are much subtler. DME effluent rises in two stages: rapidly at the beginning and then slowly until it reaches steady state. All effluent species attain steady-state at the same time. Steady-state conversion of DME into hydrocarbons is 36.7%.

The experimental data was modelled using a plug flow reactor model (equations 2.2 and 2.3) with a reaction scheme based on DFT evidence provided by Li et al. (20):

$$CH_3OCH_3 + HZ \rightleftharpoons CH_3 \cdot Z + CH_3OH \quad (S2.1)$$
$$CH_3OH + HZ \rightleftharpoons CH_3 \cdot Z + H_2O \quad (S2.2)$$
$$H_2O + HZ \rightleftharpoons H_2O \cdot HZ \quad (S2.3)$$
$$CH_3 \cdot Z + CH_3OH \rightleftharpoons CH_3OCH_3 \cdot HZ \quad (S2.4)$$
$$CH_3 \cdot Z + CH_3OCH_3 \rightarrow CH_3OCH_2 \cdot Z + CH_4 \quad (S2.5)$$
$$CH_3OCH_2 \cdot Z + CH_3OCH_3 \rightarrow CH_3OCH_2CH_2OCH_3 \cdot HZ \quad (S2.6)$$
$$CH_3OCH_2CH_2OCH_3 \cdot HZ \rightarrow CH_3CHCHOCH_3 \cdot HZ + H_2O \quad (S2.7)$$
$$CH_3CHCHOCH_3 + HZ \rightleftharpoons CH_3CHCHOCH_3 \cdot HZ \quad (S2.8)$$
$$CH_3CHCHOCH_3 + CH_3 \cdot Z \rightarrow C_3H_6 + CH_3OCH_2 \cdot Z \quad (S2.9)$$

In this scheme, steps 2.1f and 2.1b refer to the forward and backward reaction of S2.1 respectively. Figs. 2.1 and 2.2 show a comparison between experiment and simulation for the formation of propylene from DME over ZSM-5 catalysts using initial and optimised parameters respectively.

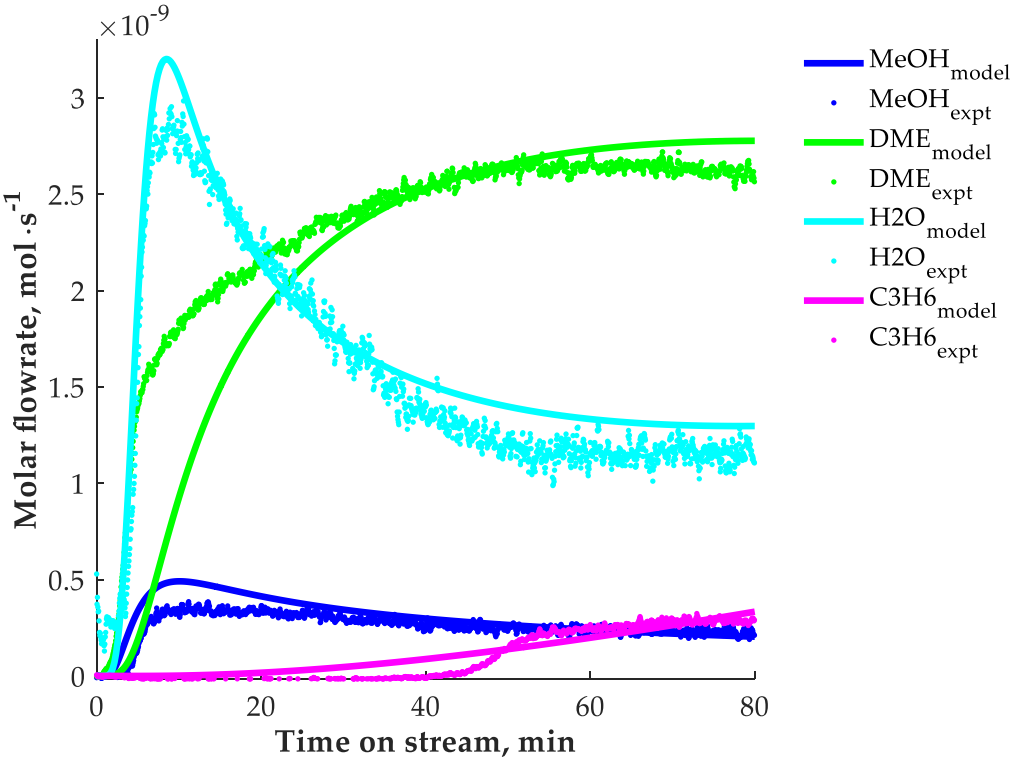

Fig. 2.1: Step response of DME over ZSM-5 catalysts at 300 °C using estimated parameters

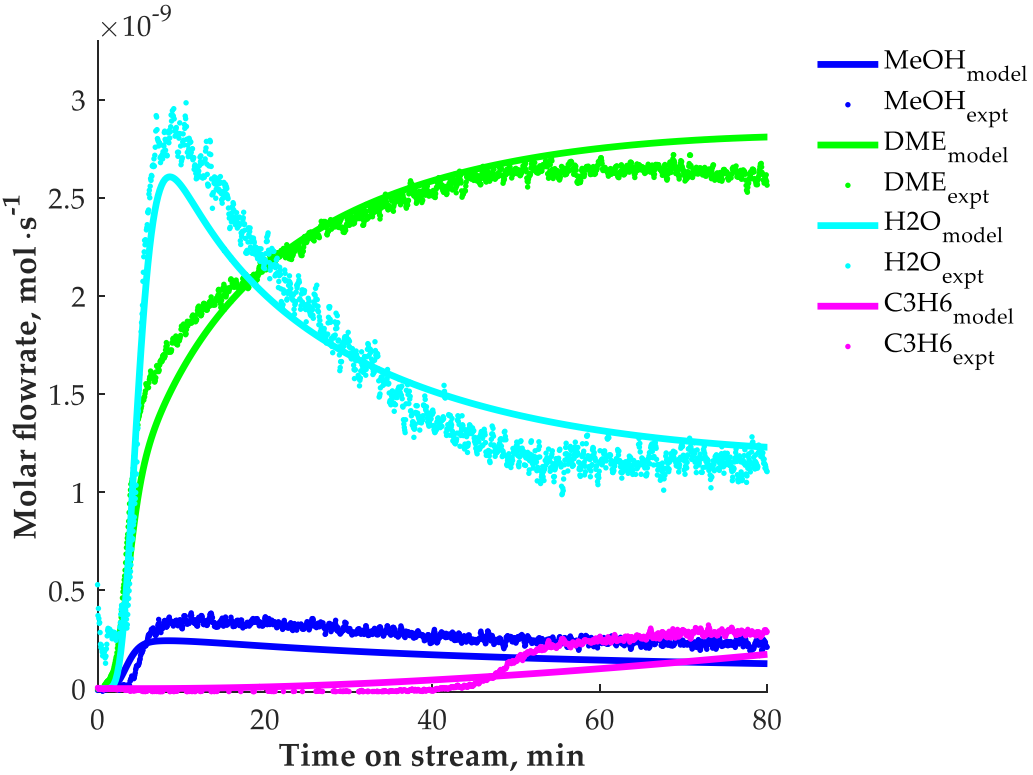

Fig. 2.2: Step response of DME over ZSM-5 catalysts at 300 °C using optimised parameters

Initial estimates used for the simulation of the experimental data are given in table 2.1. Optimised values, also given in table 2.1, were obtained by minimising the sum of squares error between experimental data and model. The sum of squares error following parameter optimization was improved by two orders of magnitude.

Table 2.1: Initial estimates and optimised parameters for the conversion of DME to propylene over ZSM-5 catalysts in a TAP reactor*

Parameters	Initial estimates	Optimised values	Unit
k_{1f}	0.0243	0.00460	$Pa^{-1}\ s^{-1}$
k_{1b}	135	35.2	$Pa^{-1}\ s^{-1}$
k_{2f}	0.014	0.0236	$Pa^{-1}\ s^{-1}$
k_{2b}	0.045	0.0450	$Pa^{-1}\ s^{-1}$
k_{3f}	0.013	0.0105	$Pa^{-1}\ s^{-1}$
k_{3b}	3	3.42	s^{-1}
k_{4f}	0.005	0.006	$Pa^{-1}\ s^{-1}$
k_{4b}	15	2.28	s^{-1}
k_{5f}	0.04	0.0786	$Pa^{-1}\ s^{-1}$
k_{6f}	4	1.18	$Pa^{-1}\ s^{-1}$
k_{7f}	2400	5347	s^{-1}
k_{8f}	0.03	0.03	$Pa^{-1}\ s^{-1}$
k_{8b}	6500	44587	s^{-1}
k_{9f}	1000	85.2	$Pa^{-1}\ s^{-1}$

*kif and kib refer to forward and backward rate constant of reaction step 2.i.

Sensitivity analysis was carried out using equation 2.6. It can be observed that steps S2.1, S2.2, S2.3, S2.5 and S2.6 are the most important elementary steps during the formation of propylene from DME using the reaction scheme depicted in section 4.1.

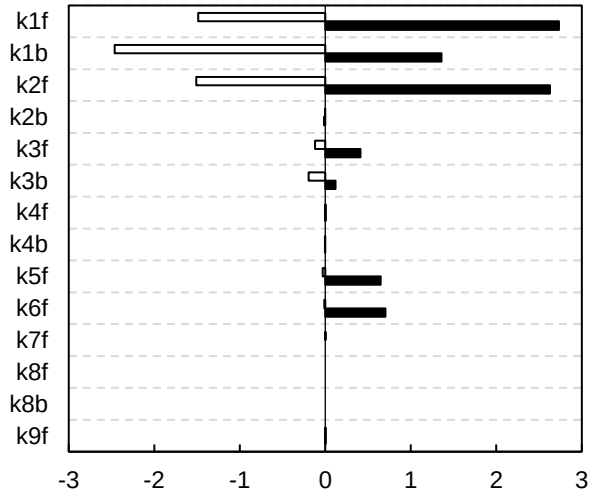

Fig. 2.3: Sensitivity analysis for elementary steps involved in the formation of propylene from DME over ZSM-5 catalysts at 300 °C

5. Discussion

The debate on the formation of primary olefins is focused on advancing understanding on the mechanism through which the key oxygenate transforms during the induction period. This contribution has focused on the chemical kinetics through which DME transforms to the propylene under TAP conditions at 300 °C. A focus on the chemical kinetics would help elucidate the major bottlenecks involved in propylene formation. Ultimately this study fits within the larger framework of quantitatively describing the evolution of the hydrocarbon pool mechanism that subsequently regulates product distribution over zeolite and zeotype catalysts at steady-state. It is a step-forward towards further elucidation on the effects of hydrodynamics and transport artefacts when reactor scale-up is considered.

The adsorption and desorption of DME, methanol and water as well as the reaction of surface methoxy groups and methanol govern their initial release into the gas phase and the early concentrations of methoxy groups on the catalyst surface. The desorption of DME is much faster than its adsorption and the desorption of methanol is faster than its adsorption. DME desorption is two orders of magnitude faster than methanol desorption under reactive conditions. Gaseous DME reacts with surface methoxy groups and methoxy methyl groups in reaction steps 2.5 and 2.6 to produce methoxy methyl groups and dimethoxyethane respectively. The higher reverse dissociation rate (i.e. association rate) of gaseous DME (step 2.1) on the active site is necessary to supply its gaseous form needed for reactions later (steps 2.5 and 2.6) in the induction period. In Figs. 2.1 and 2.2, DME effluent reaches its steady state value slowly following an initial rapid rise. The initial rapid rise is because the rate of reaction

of surface methoxy groups and methanol is much slower than their formation in step 2.4f together with a fast backward rate constant in step 2.1 leading to large releases of DME into the gas phase. The slower rate of rise following afterwards is due to the reactions involving DME in steps 2.5 and 2.6 later during the induction period.

Surface methoxy groups are generated early in the induction period and consumed later leading to the formation of intermediates and propylene. According to the scheme, there is a rather slow generation of surface methoxy groups given by the dissociation rates of DME and methanol in reaction steps 2.1f and 2.2f respectively. Surface methoxy groups are also slowly consumed leading to the formation of adsorbed DME (steps 2.4f) and generation of methoxy methyl groups (step 2.5f). However, they are rapidly consumed in step 2.9f leading to the formation of propylene. Surface methoxy groups are slowly generated and rapidly consumed during the induction period.

The water effluent is controlled by its adsorption and desorption (step 2.3) and the adsorption and desorption of methanol (step 2.2) and the formation of methyl propenyl ether from dimethoxyethane (step 2.7). Methanol adsorption and desorption leads to small concentrations of water in the gas phase (step 2.2). Once formed, water remains mostly in the gas phase (step 2.3). Step 2.7f shows a large reaction rate constant for the formation of water effluent from dimethoxyethane. Water effluent portrays an overshoot profile with time on stream. Although it is rapidly produced in steps 2.7f and rapidly desorbed in step 2.3b, it reacts rapidly with methoxy groups to give methanol in step 2.2b. Thus, the overshoot in water effluent is due to the competing dynamics governing its formation and consumption during the induction period.

Gaseous methanol effluent is affected by the early reactions (steps 2.1, 2.2 and 2.4). Desorption rates greater than adsorption rates lead to a slow release of methanol in the gas phase following steps 2.1 and 2.2. In step 2.4f, methanol is slowly consumed, although the rate of reaction is slower than its nominal formation rate in steps 2.1 and 2.2. Thus, in steps 2.1 and 2.2, small concentrations of methanol are generated which are slowly consumed in step 2.4 during the induction period. The difference between the rates of methanol formation and consumption is responsible for its slight overshoot depicted in Fig. 2.1. Methanol overshoot effectively mirrors water overshoot except its features are subtler. Reaction step 2.2. connects methanol, water and surface methoxy groups. The generation of surface methoxy groups is one of the slower steps in the overall reaction; a factor resulting in an overshoot as described by Kobayashi et al. (30, 31).

Propylene is formed very rapidly (step 2.9f) from the initial species (methanol, DME, water, surface methoxy groups, methoxymethyl groups) through a series of intermediates (dimethoxyethane and methyl propenyl ether). Both intermediates are readily available in the pores of the ZSM-5 catalyst (dimethoxyethane) and in the gas phase due to high desorption

rates (methyl propenyl ether). The bottleneck (limiting step) in propylene formation, given the initial species, is the formation of dimethoxyethane from gaseous DME and methoxymethyl groups in step 2.6. Step 2.6 represents the formation of the first C-C bond during propylene formation from DME. It is also a very important elementary step according to the sensitivity analysis given in Fig. 2.3. The S-shaped profile is due to the slow transformation of several stable intermediates (30) such as surface methoxy groups, methoxymethyl groups, methyl propenyl ether. Methoxy methyl groups serve as autocatalysing species as they are generated in step 2.5, consumed in step 2.6 and regenerated in step 2.9 consequently leading to the S-shaped profile observed by propylene effluent.

6. Conclusions

The formation of primary olefins from dimethyl ether (DME) has been studied over ZSM-5 catalyst using a step response methodology in a temporal analysis of products (TAP) reactor. Propylene is the major olefin formed at 300 °C and portrays an S-shaped profile. Overshoot profiles are depicted by methanol and water with time on stream. DME effluent reaches its steady state flowrate in two phases: rapidly and then slowly. The results were explained using a kinetic model based on a reaction scheme based on recent Density Functional Theory studies. After the formation of primary products (methanol, water, surface methoxy groups, methoxymethyl groups and methane) from DME, the formation of the first C-C bond (reaction of methoxymethyl group with DME to give dimethoxyethane) represents the major bottleneck in propylene formation.

7. References

1. Tian P, Wei Y, Ye M, Liu Z. Methanol to olefins (MTO): From fundamentals to commercialization. ACS Catalysis. 2015;5(3):1922-38.
2. Dahl IM, Kolboe S. On the reaction mechanism for propene formation in the MTO reaction over SAPO-34. Catal Lett. 1993;20(3-4):329-36.
3. Dahl IM, Kolboe S. On the Reaction Mechanism for Hydrocarbon Formation from Methanol over SAPO-34. I. Isotopic Labeling Studies of the Co-Reaction of Ethene and Methanol. J Catal. 1994;149(2):458-64.
4. Dahl IM, Kolboe S. On the reaction mechanism for hydrocarbon formation from methanol over SAPO-34: 2. Isotopic labeling studies of the Co-reaction of propene and methanol. J Catal. 1996;161(1):304-9.
5. Olsbye U, Bjørgen M, Svelle S, Lillerud KP, Kolboe S. Mechanistic insight into the methanol-to-hydrocarbons reaction. International Conference on Gas-Fuel 05. 2005;106(1-4):108-11.
6. Bjørgen M, Svelle S, Joensen F, Nerlov J, Kolboe S, Bonino F, Palumbo L, Bordiga S, Olsbye U. Conversion of methanol to hydrocarbons over zeolite H-ZSM-5: On the origin of the olefinic species. J Catal. 2007;249(2):195-207.
7. Ilias S, Bhan A. Mechanism of the catalytic conversion of methanol to hydrocarbons. ACS Catalysis. 2013;3:18-31.

8. Svelle S, Kolboe S, Swang O, Olsbye U. Methylation of Alkenes and Methylbenzenes by Dimethyl Ether or Methanol on Acidic Zeolites. The Journal of Physical Chemistry B. 2005;109(26):12874-8.
9. Stöcker M. Methanol-to-hydrocarbons: Catalytic materials and their behavior. Microporous Mesoporous Mater. 1999;29(1-2):3-48.
10. Lesthaeghe D, Van Speybroeck V, Marin GB, Waroquier M. Understanding the failure of direct C-C coupling in the zeolite-catalyzed methanol-to-olefin process. Angewandte Chemie - International Edition. 2006;45(11):1714-9.
11. Lesthaeghe D, Van Speybroeck V, Marin GB, Waroquier M. What role do oxonium ions and oxonium ylides play in the ZSM-5 catalysed methanol-to-olefin process? Chem Phys Lett. 2006;417(4-6):309-15.
12. Lesthaeghe D, Van Speybroeck V, Marin GB, Waroquier M. The rise and fall of direct mechanisms in methanol-to-olefin catalysis: An overview of theoretical contributions. Ind Eng Chem Res. 2007;46(26):8832-8.
13. Goguen PW, Xu T, Barich DH, Skloss TW, Song W, Wang Z, Nicholas JB, Haw JF. Pulse-quench catalytic reactor studies reveal a carbon-pool mechanism in methanol-to-gasoline chemistry on zeolite HZSM-5. J Am Chem Soc. 1998;120(11):2650-1.
14. Song W, Marcus DM, Fu H, Ehresmann JO, Haw JF. An oft-studied reaction that may never have been: Direct catalytic conversion of methanol or dimethyl ether to hydrocarbons on the solid acids HZSM-5 or HSAPO-34. J Am Chem Soc. 2002;124(15):3844-5.
15. Wang W, Seiler M, Hunger M. Role of surface methoxy species in the conversion of methanol to dimethyl ether on acidic zeolites investigated by in situ stopped-flow MAS NMR spectroscopy. J Phys Chem B. 2001;105(50):12553-8.
16. Wang W, Buchholz A, Seiler M, Hunger M. Evidence for an Initiation of the Methanol-to-Olefin Process by Reactive Surface Methoxy Groups on Acidic Zeolite Catalysts. J Am Chem Soc. 2003;125(49):15260-7.
17. Jiang Y, Wang W, Marthala VRR, Huang J, Sulikowski B, Hunger M. Effect of organic impurities on the hydrocarbon formation via the decomposition of surface methoxy groups on acidic zeolite catalysts. J Catal. 2006;238(1):21-7.
18. Chowdhury AD, Houben K, Whiting GT, Mokhtar M, Asiri AM, Al-Thabaiti SA, Basahel SN, Baldus M, Weckhuysen BM. Initial Carbon–Carbon Bond Formation during the Early Stages of the Methanol-to-Olefin Process Proven by Zeolite-Trapped Acetate and Methyl Acetate. Angewandte Chemie - International Edition. 2016;55(51):15840-5.
19. Liu Y, Müller S, Berger D, Jelic J, Reuter K, Tonigold M, Sanchez-Sanchez M, Lercher JA. Formation Mechanism of the First Carbon-Carbon Bond and the First Olefin in the Methanol Conversion into Hydrocarbons. Angewandte Chemie - International Edition. 2016;55(19):5723-6.
20. Li J, Wei Z, Chen Y, Jing B, He Y, Dong M, Jiao H, Li X, Qin Z, Wang J, Fan W. A route to form initial hydrocarbon pool species in methanol conversion to olefins over zeolites. J Catal. 2014;317(0):277-83.
21. Omojola T, Cherkasov N, McNab AI, Lukyanov DB, Anderson JA, Rebrov EV, van Veen AC. Mechanistic Insights into the Desorption of Methanol and Dimethyl Ether Over ZSM-5 Catalysts. Catal Lett. 2018;148(1):474-88.
22. Wei Z, Chen YY, Li J, Guo W, Wang S, Dong M, Qin Z, Wang J, Jiao H, Fan W. Stability and Reactivity of Intermediates of Methanol Related Reactions and C-C Bond Formation over H-ZSM-5 Acidic Catalyst: A Computational Analysis. Journal of Physical Chemistry C. 2016;120(11):6075-87.
23. Gleaves JT, Ebner JR, Kuechler TC. Temporal Analysis of Products (TAP) — A Unique Catalyst Evaluation System with Submillisecond Time Resolution. Catalysis Reviews. 1988;30(1):49-116.
24. Hinrischen O, van Veen AC, Zanthoff HW, Muhler M. TAP Reactor Studies. In: Haw JF, editor. In-Situ Spectroscopy in Heterogeneous Catalysis. WeinHeim: Wiley-VCH; 2002.

25. Shekhtman SO, Yablonsky GS, Chen S, Gleaves JT. Thin-zone TAP-reactor - theory and application. Chem Eng Sci. 1999;54(20):4371-8.
26. Gleaves JT, Yablonsky G, Zheng X, Fushimi R, Mills PL. Temporal analysis of products (TAP)—Recent advances in technology for kinetic analysis of multi-component catalysts. J Mol Catal A: Chem. 2010;315(2):108-34.
27. Marin GB, Yablonsky GS. Kinetics of Chemical Reactions: Decoding Complexity Weinheim, Germany: WILEY-VCH; 2011. 1-428.
28. Courant R, Friedrichs K, Lewy H. Über die partiellen Differenzengleichungen der mathematischen Physik. Mathematische Annalen. 1928;100(1):32-74.
29. Lagarias JC, Reeds JA, Wright MH, Wright PE. Convergence properties of the Nelder-Mead simplex method in low dimensions. SIAM Journal on Optimization. 1998;9(1):112-47.
30. Kobayashi M. Characterization of transient response curves in heterogeneous catalysis—I Classification of the curves. Chem Eng Sci. 1982;37(3):393-401.
31. Kobayashi M. Characterization of transient response curves in heterogeneous catalysis - 2. Estimation of the reaction mechanism in the oxidation of ethylene over a silver catalyst from the mode of the transient response curves. Chem Eng Sci. 1982;37(3):403-9.